Pergamon

Bioorganic & Medicinal Chemistry 7 (1999) 1145–1150

BIOORGANIC & MEDICINAL CHEMISTRY

A Comparison of Flexible and Constrained Haptens in Eliciting Antibody Catalysts for Paraoxon Hydrolysis

David A. Spivak, Timothy Z. Hoffman, Alisa H. Moore, Matthew J. Taylor and Kim D. Janda*

The Scripps Research Institute, Department of Chemistry and The Skaggs Institute for Chemical Biology, 10550 North Torrey Pines Road, La Jolla, CA, 92037, USA

Received 11 November 1998; accepted 16 December 1998

Abstract—A new amine-oxide hapten was employed as an antigen, producing seven monoclonal antibodies (mAbs) from a panel of 20 that catalyzed paraoxon hydrolysis. The current hapten design differs from that previously described in that the molecule is inherently more flexible than its constrained predecessor. One of the seven antibody catalysts, mAb 1H9, showed the highest activity and was selected for detailed study. At pH = 8.77, the catalytic hydrolysis of paraoxon by mAb 1H9 followed Michaelis–Menten kinetics affording a $k_{cat} = 3.73 \times 10^{-4}\,min^{-1}$ and a $K_m = 1.12\,mM$ with a rate acceleration $k_{cat}/k_{uncat} = 56$. The hapten was found to be a competitive inhibitor of antibody-catalyzed paraoxon hydrolysis with a $K_i = 0.54\,mM$. A comparison of both the number and proficiency of antibody catalysts obtained when utilizing a flexible versus constrained hapten indicates that, for paraoxon hydrolysis, constrained haptens elicit superior catalysts, suggesting that further development should begin with the use of constrained haptens in producing more proficient antibody catalysts for paraoxon hydrolysis.

Introduction

Phosphotriester containing compounds such as paraoxon, parathion, and diazinon have been widely used as commercial insecticides (Fig. 1). These compounds act by inhibiting acetylcholinesterase, the enzyme responsible for regulating the concentration of the neurotransmitter acetylcholine.[1] In addition to insect control, phosphotriesters can also poison mammalian systems as well.[1] As a result, structural variants of phosphotriesters have been developed as potent biological warfare agents. These compounds, such as sarin and soman, are referred to as G-series nerve agents or their surrogates such as DFP (Fig. 2). Methods for the selective neutralization of these phosphotriesters would be of great value as both protective measures[2–5] and therapeutic treatments.[1]

Background and Significance

There is considerable interest in developing biocatalysts for the degradation of phosphotriester derived insecticides and warfare agents.[2–6] At present, there is one known type of phosphotriesterase which utilizes two zinc ions to effect catalysis.[7,8] Although phosphotriesterases exist in nature, their natural substrates have not been identified.[9] In addition to natural phosphotriesterase, mutated buCHE (butyryl cholinesterase) and DFPase are being developed for hydrolysis of phosphotriesters and their derivatives.[2]

In addition to enzyme strategies, antibody catalysts could in theory be employed for decontamination of toxic phosphotriesters and their structural variants. Unlike enzymes that provide for evolutionary determined substrates, antibodies can be tailored for specific binding and catalytic properties. Antibodies can also be utilized for in vivo as well as in vitro applications. For example, antibodies have been used therapeutically to treat exposure to snake venoms[10] and cocaine[11] by binding the toxic substances and isolating them from susceptible tissues. An alternative approach to immunotherapy can be envisioned by the utilization of antibody catalysts that decompose the toxin of interest rather than simply sequestering it. As part of a program directed toward antibody mediated phosphotriester hydrolysis, we have focused on developing catalytic antibodies for the hydrolysis of paraoxon.[12–14]

Antibodies that hydrolyze carboxylate esters have been elicited against compounds that mimic the tetrahedral transition state of the respective reactions.[15–18] In contrast, the analogous phosphotriester hydrolysis occurs through a trigonal bipyramidal pentacoordinate transition state intermediate. The pentacoordinate transition

*Corresponding author. Tel.: 619-784-2516; fax: 619-784-2595; e-mail: kdjanda@scripps.edu

0968-0896/99/$ - see front matter
PII: S0968-0896(99)00026-7

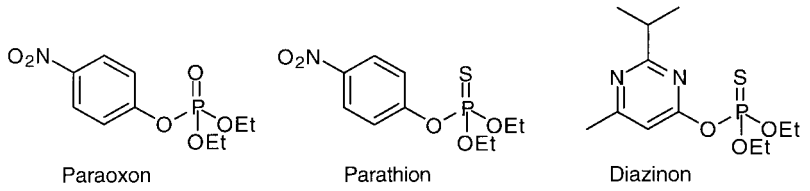

Figure 1. Representative phosphotriester insecticides.

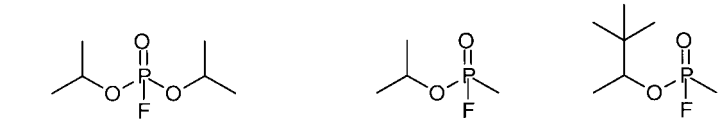

Figure 2. Representative G-series nerve agents and their surrogates.

state arises from attack of hydroxide and in-line displacement of the leaving group in apical positions.[19–21] Although the tetrahedral intermediate of carboxylate ester hydrolysis is accurately mimicked by many transition state analogues,[22,23] functionality representing pentavalent centers[24,25] are less common due to instability or toxicity. The electrostatic features of the phosphotriester hydrolysis transition state anticipated along the reaction coordinate, however, are more easily mimicked. Through a strategy known as 'bait and switch' catalysis, it has been previously shown that charged haptens can induce complementary antibodies that can catalyze hydrolysis by stabilization of a polar transition state, or by eliciting a side chain group capable of acid–base interactions.[26–29]

Using the principle of hapten-charge complementarity, it was found that either amine-oxide or quaternary amine based haptens elicit antibodies with phosphotriesterase activity.[12–14] Initially, the best antibody catalysts were induced by haptens incorporating an amine-oxide center versus the quaternary amine functionality.[12] This was presumably due to the ability of the *N*-oxide to induce antibodies that not only complemented the partial positive character of the phosphorous center, but stabilized the developing negative charge at the leaving-group oxygen as well. In a subsequent report, paraoxon was found to be hydrolyzed by an antibody elicited to compound **1** (Fig. 3), which contained the 4-nitrophenyl group and the alkyl groups constrained in a six-membered ring.[13,14] The results gave a rate acceleration (k_{cat}/k_{uncat}) of approximately 500, providing a foundation for the development of more proficient antibody catalysts for this hydrolysis reaction.

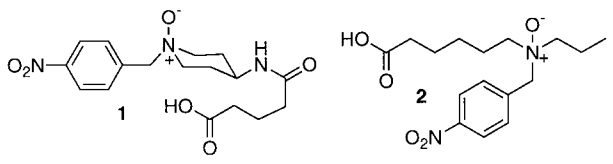

Figure 3. The constrained hapten **1**, previously employed to obtain antibody catalysts for the hydrolysis of paraoxon, and the more flexible hapten **2** used in the current study.

In an attempt to obtain antibody catalysts with improved rates of catalysis, hapten **2** was designed as a more faithful representation of the paraoxon structure (Fig. 3). The linker itself incorporates a steric mimic of one ethyl ester of paraoxon and the propyl group mimics the other. An important feature was the absence of the six-membered ring, which may increase the flexibility of the entire structure, allowing a variety of binding and recognition modes. It was unknown, however, what affect this change would have on the elicitation of antibody catalysts. It was hoped that a more flexible hapten would induce more proficient catalysts, though in any event a comparison with our previous studies may provide for future directions in this area.

Results and Discussion

Hapten **2** was synthesized in four steps as described in Scheme 1. Reductive amination of 6-amino caproic acid *n*-hexyl ester with propionaldehyde gave the secondary amine **3**. Saponification followed by alkylation with 4-nitrobenzyl bromide gave the amino acid **5**. Lastly, oxidation of the amine with mCPBA gave the hapten **2**, which was conjugated to keyhole limpet hemocyanin (KLH) for immunization.[30]

A total of 20 monoclonal antibodies were obtained that bound specifically to hapten **2** as determined by enzyme-linked immunosorbent assay (ELISA). Seven antibodies were found to accelerate the hydrolysis of paraoxon with varying degrees of activity. One of these, mAb 1H9, showed the highest activity and was selected for detailed study. The catalytic hydrolysis of paraoxon by mAb 1H9 followed Michaelis–Menten kinetics and displayed turnover, affording k_{cat} values ranging from $1.21\times10^{-4}\,min^{-1}$ to $1.25\times10^{-3}\,min^{-1}$ in the pH range 8.0–10.0. Importantly, at a pH of 9.0, hapten analogue **7** (Scheme 2) was a competitive inhibitor of antibody 1H9 with a K_i of 0.54 mM. Hapten analogue **7** was synthesized by alkylation of dipropylamine with 4-nitrobenzyl bromide to give intermediate **6**, followed by oxidation with mCPBA (Scheme 2).

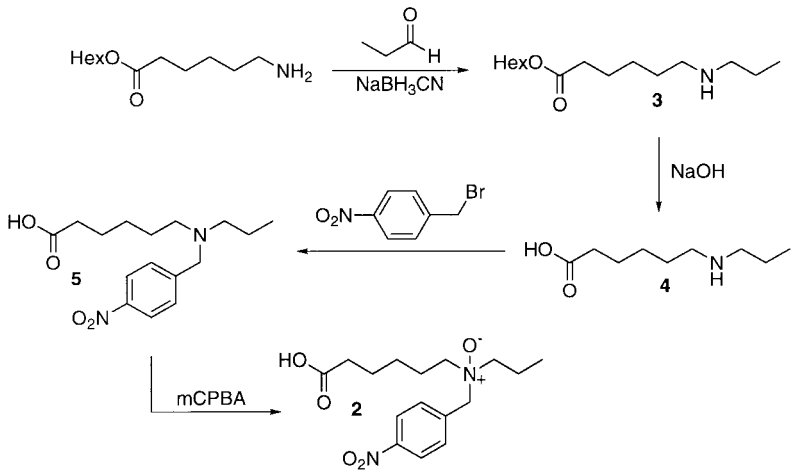

Scheme 1. Synthesis of *N*-oxide hapten **2**.

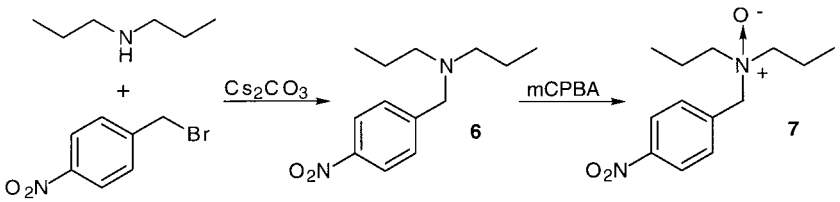

Scheme 2. Synthesis of hapten analogue **7** used to determine K_i with mAb 1H9.

The pH profile of catalytic hydrolysis of paraoxon by mAb 1H9 showed a linear dependence of log k_{cat} on the concentration of hydroxide ion from pH 8–10 (Fig. 4).

This pH dependence was similar to that seen for antibody 3H5.[14] Additionally, the uncatalyzed rate of paraoxon hydrolysis was also found to be linearly dependent on hydroxide concentration. These observations argued against general acid–base catalysis, because no titratable pK_a (apparent) was observed in the log k_{cat} versus pH plot, and may suggest that antibody catalysis was operating through stabilization of the transition state. Transition state stabilization could occur through complementarity of the antibody combining site to the developing positive charge on the phosphorous center. Electrostatic stabilization of the positive phosphorous center could be achieved with an ionized Glu or Asp amino acid side chain carboxylate (pK_a less than 5.0) in the combining site. In addition, amino acids with positively charged side chains (e.g. Arg or Lys) may also stabilize either the developing negative charge on the leaving group oxygen atom or the partial negative charge on the phosphoryl oxygen atom in the transition state for paraoxon hydrolysis. These interactions would be expected to lower the energy of the charged transition state for phosphotriester hydrolysis in the antibody combining site and may have led to the observed rate acceleration. A comparison of K_m/K_i (2.1) with k_{cat}/k_{uncat} (56), however, indicated that other effects besides transition-state stabilization were present. The value K_m/K_i is typically taken to approximate the rate acceleration attainable by transition-state stabilization alone,[31] but the observed rate acceleration clearly exceeds this value. Perhaps general-base catalysis by an amino acid side chain possessing a pK_a outside the pH range shown in Figure 4 is utilized by mAb 1H9.

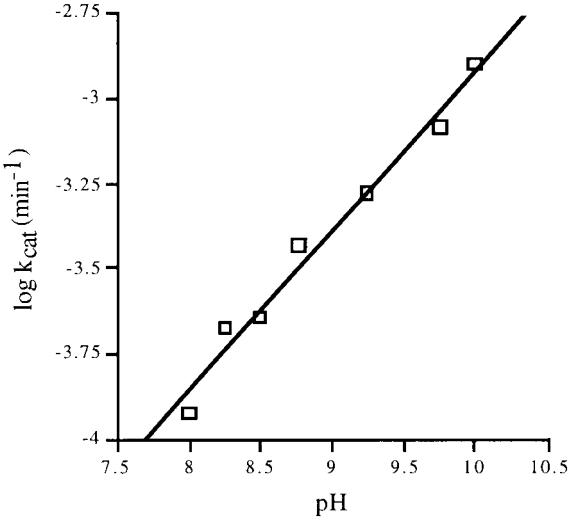

Figure 4. Dependence of log k_{cat} antibody 1H9 catalyzed paraoxon hydrolysis on pH.

Substrate specificity was assessed utilizing two compounds that are structurally similar to paraoxon and the hapten (Fig. 5). Compound **8** was synthesized by stepwise addition of 4-nitrophenol, then 1-butanol to ethyl dichlorophosphate. Compound **9** was obtained by

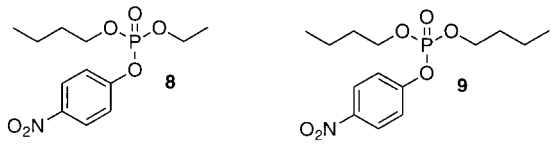

Figure 5. Compounds employed to determine specificity of hydrolytic activity by mAb 1H9.

bis-condensation of 4-nitrophenyl phosphorodichloridate. Both compounds **8** and **9** are homologous to paraoxon and, as a result, mAb 1H9 was found to catalyze the hydrolysis of **8** and **9**. A quantitative measure of substrate specificity is k_{cat}/K_m (Table 1).

For paraoxon, $k_{cat}/K_m = 4\times10^{-4}$ at pH 9.0. This is approximately five fold lower than for compound **8**, showing little difference in substrate specificity due to a change in one alkyloxy substituents. However, for compound **9** a 100-fold decrease in k_{cat}/K_m was observed relative to that for compound **8**, suggesting higher specificity for the ethyl/butyl versus butyl/butyl substituted phosphotriester. As in the case of antibody 3H5, the aromatic nitro group is most likely the primary recognition element for the antibody,[14] though it is clear that the aliphatic substituents are also important determinants for antibody-substrate binding and catalysis.

The design of efficient biocatalytic hydrolysis of phosphotriesters and their derivatives is currently an important goal for both in vitro and in vivo applications. In this report, hapten **2** provided seven antibody catalysts for the hydrolysis of paraoxon. The best of these antibodies, 1H9, provided a rate acceleration of 56, 10-fold lower than the previous report.[14] The differences in performance between antibody 3H5 and 1H9 may be related to differences in hapten design. The design of hapten **2** incorporated a more faithful representation of the ground state paraoxon structure and provided structural flexibility for a variety of binding and recognition modes. This structural flexibility may be responsible for the high number of antibody catalysts (seven out of 20) elicited to hapten **2** for paraoxon hydrolysis as compared to hapten **1** (one out of 25). Alternatively, the more conformationally restricted alkyl groups of hapten **1** may have provided a better steric mimic of the trigonal bipyramidal transition state of paraoxon hydrolysis, affording an antibody catalyst with a higher rate acceleration (500 versus 56). Perhaps most importantly, the geometric constraints in hapten **1** may also provide ground state strain for paraoxon hydrolysis. With regard to this issue, a relevant comparison can be found in the small difference in $\Delta\Delta H$ (1.2 kcal/mol) of hydrolysis for the cyclic trimethylene phosphate versus the acyclic dimethyl phosphate, where ring strain was found to destabilize the ground state energy of the cyclic phosphodiester.[32] Though it is unknown at this time whether this is a general phenomenon, it is clear in this case that the constrained hapten generated fewer, but more proficient antibody catalysts than its flexible counterpart. This will therefore represent a starting point for improvements in the antibody-catalyzed hydrolysis of paraoxon. Both examples, however, support the theory that amine-oxides provide crucial hapten-charge complementarity for lowering the energy of the developing charges in the transition state for phosphotriester hydrolysis reactions.

Experimental

General

6-Amino-*n*-caproic acid *n*-hexyl ester *p*-toluenesulfonate was purchased from TCI Chemicals. Paraoxon (90%) was obtained from Aldrich Chemicals and then purified by flash chromatography using EtOAc:hex (50:50) as eluant. Flash chromatography was carried out using Mallinckrodt silica gel 60 (230–400 mesh). Preparative TLC was performed with Merck glass plates coated with 1.0 mM silica. HPLC separations were carried out on a Rainin Preparative HPLC using a Vydac reverse phase C18 90Å pharmaceutical column. ^1H and ^{13}C NMR spectra were obtained on Bruker 300 mHz or 500 mHz instruments. Chromatographic and reagent solvents were reagent grade and used as received. All reagents were obtained from commercial sources and were used without further purification.

Antibody preparation

Hapten **2** was coupled to keyhole limpet hemocyanin (KLH) and bovine serum albumin using 1-[3-(dimethylamino)propyl]-3-ethylcarbodiimide hydrochloride (EDC) as previously reported.[33] Mice were immunized with the KLH conjugate of **2**, and monoclonal antibodies were obtained using standard procedures.[30] Antibody 1H9 was purified via DEAE anion exchange chromatography, Protein G affinity chromatography, and Mono Q anion exchange chromatography and was demonstrated to be >98% homogeneous by SDS acrylamide gel electrophoresis.

Assays

All paraoxon hydrolysis reactions, as well as for compound **8,** were performed in 96-well microtiter plates containing 235 μL of CHES buffer with 20 μM antibody and 2.5% DMSO. For these hydrolysis reactions,

Table 1. Comparison of kinetic parameters for antibody 1H9 catalyzed hydrolysis of compounds **8**, **9**, and paraoxon at various pH values

Substrate	pH	k_{uncat} (min^{-1})	k_{cat} (min^{-1})	K_m (mM)	k_{cat}/K_m
Paraoxon	8.77	6.62×10^{-6}	3.73×10^{-4}	1.12	3.33×10^{-4}
Paraoxon	9.25	1.20×10^{-5}	5.36×10^{-4}	1.06	5.06×10^{-4}
8	9.00	4.32×10^{-5}	1.09×10^{-3}	0.44	2.48×10^{-3}
8	9.25	9.00×10^{-5}	1.25×10^{-3}	0.28	4.46×10^{-3}
9	9.00	1.48×10^{-6}	3.84×10^{-5}	1.03	3.73×10^{-5}

kinetic assays for the release of *p*-nitrophenol were performed at 25 °C on a Molecular Devices Thermomax ELISA plate reader measured at $\lambda = 405$ nm for detection of 4-nitrophenolate. For each pH, kinetic parameters were obtained from the average of two runs using substrate concentrations between 500 μM and 5.0 mM of paraoxon. Calibration curves for the absorbance of 4-nitrophenol were obtained for each pH. Assays for the hydrolysis of compound **9** were carried out on a Hitachi HPLC using a VYDAC 201TP504 reverse phase column. The mobile phase used was CH_3CN:H_2O (34:66) (0.1% TFA) at a flow rate of 1.0 mL/min with UV detection at $\lambda = 320$ nm. Dixon plot experiments showed the paraoxon analogue **7** to be a competitive inhibitor of paraoxon hydrolysis by antibody 1H9.

6-*N*-Propylamino caproic acid *n*-hexyl ester (3). 6-Amino-*n*-caproic acid *n*-hexyl ester (2.08 g, 9.7 mmol), propionaldehyde (0.78 g, 13.5 mmol), and acetic acid (1.18 g, 19.3 mmol) were dissolved in 30.0 mL of MeOH, followed by addition of 0.05 g 3 angstrom molecular sieves. Sodium cyanoborohydride was added in one portion and the reaction mixture was stirred at rt for 48 h. The reaction mixture was brought to pH = 2 slowly using concentrated HCl with concomitant evolution of gas. After gas evolution stopped, the solution was brought to pH = 13 using solid sodium hydroxide. Methanol was removed by rotary evaporation, and the remaining aqueous layer extracted with Et_2O (3×50 mL). The organic layers were combined and washed with saturated aqueous sodium chloride (1×50 mL), dried over Na_2SO_4, and evaporated under reduced pressure. Purification by flash chromatography using MeOH as eluant gave 0.41 g (16%) of **3** as a clear residue. ^{1}H NMR (300 mHz, CD_3OD): δ 4.04 (t, $J = 6$ Hz, 2H), 3.65 (s, 1H), 2.57 (m, 4H), 2.31 (t, $J = 9$ Hz, 2H), 1.63 (m, 4H), 1.49 (m, 4H), 1.34 (m, 8H), 0.89 (m, 6H); ^{13}C NMR (75 MHz, CD_3OD): δ 173.7, 64.3, 51.8, 49.6, 34.1, 31.3, 29.7, 28.4, 26.8, 25.4, 24.7, 23.0, 22.4, 13.8, 11.6; HRMS (FAB^+): calcd 257.2355, found 257.2350.

6-*N*-Propylamino caproic acid (4). Amine **3** (0.17 g, 0.66 mmol) was dissolved in 1.5 mL MeOH, and an equal volume of 1M NaOH was added. After stirring for 1 h, the reaction mixture was purified directly by flash chromatography using MeOH as the eluant to give 0.13 g (94%) of **4** as a white solid. ^{1}H NMR (300 mHz, CD_3OD): δ 3.11 (s, 1H), 2.67–2.75 (m, 4H), 2.23 (t, $J = 7$ Hz, 2H), 1.34–1.54 (m, 6H), 0.78 (t, $J = 7$ Hz, 3 H); ^{13}C NMR (75 MHz, CD_3OD): δ 165.7, 42.1, 40.5, 25.2, 24.4, 17.0, 15.5, 10.7; HRMS (FAB^+): calcd 173.1416, found 173.1418.

6-[*N*-(4-Nitrobenzyl)-*N*-propyl]-amino caproic acid (5). Amino acid **4** (0.07 g, 0.4 mmol) was dissolved in 3.0 mL MeOH. Triethylamine (0.14 mL, 1.0 mmol) and 4-nitrobenzyl bromide (0.11, 0.5 mmol) were added and the reaction stirred for 48 h. The reaction was evaporated under pressure, and the product purified by preparative TLC using two eluants: first with a EtOAc:hex (50:50) mixture, then with pure EtOAc. This afforded 0.03 g (22%) of **5** as a yellow oil. ^{1}H NMR (300 MHz, CD_3OD): δ 8.14 (d, $J = 9$ Hz, 2H), 7.47 (d, $J = 9$ Hz, 2 H), 3.59 (s, 2H), 2.31–2.40 (m, 4H), 2.26 (t, $J = 8$ Hz, 2H), 1.52–1.62 (m, 2H), 1.39–1.49 (m, 4H), 1.23–1.32 (m, 4 H), 0.83 (t, $J = 8$ Hz, 3H), ^{13}C NMR (75 mHz, CD_3OD): δ 174.2, 148.8, 133.9, 129.1, 123.4, 58.3, 56.1, 53.9, 34.0, 29.7, 26.9, 24.8, 20.3, 11.8; HRMS (FAB^+): calcd 308.2006, found 308.1942.

6-[*N*-(4-Nitrobenzyl)-*N*-propyl-*N*-oxido]-amino caproic acid (2). Amino acid **5** (0.02 g, 0.07 mmol) was suspended in 1.0 mL CH_2Cl_2. After mCPBA (60–70%, 0.022 g, 0.07 mmol) was added, the mixture was shaken on a vortex machine for 30 min. The CH_2Cl_2 was evaporated under reduced pressure, and the residue triturated with Et_2O to leave 12 mg of a white solid. The solid was purified by reversed phase HPLC (flow rate = 1.0 mL/min, $\lambda = 254$) using a 35:65 ratio of MeCN:H_2O as eluant. The product eluted at 7.5 min, and lyophilization gave 7.5 mg (36%) of pure **2** as a clear oil. ^{1}H NMR (300 MHz, CD_3OD): δ 8.25 (d, $J = 9$ Hz, 2H), 7.72 (d, $J = 9$ Hz, 2H), 4.80 (s, 2H), 3.35–3.42 (m, 4H), 2.10 (t, $J = 7$ Hz, 2H), 1.77–1.86 (m, 4H), 1.57 (tt, $J = 8$ Hz, 7 Hz, 2H), 1.27–1.34 (m, 2H), 0.90 (t, $J = 7$ Hz, 3H); ^{13}C NMR (75 mHz, CD_3OD): δ 150.7, 135.4, 132.2, 124.9, 68.1, 66.8, 65.2, 34.3, 26.9, 26.5, 25.5, 23.4, 17.3, 11.2, 10.6; HRMS (FAB^+): calcd 324.1685, found 324.1677.

***N*-(4-Nitrobenzyl)-dipropyl amine (6).** Dipropylamine (3.39 mL, 24.7 mmol) and 4-nitrobenzyl bromide (8.21 g, 38 mmol) were dissolved in 27 mL of DMF. Cesium carbonate (12.38 g, 38 mmol) was added and the mixture stirred 1 h. at 0 °C, then 3 h at room temperature. The reaction mixture was diluted with 5 equiv of H_2O, then extracted with EtOAc (3×100 mL). The organic layers were combined, washed with aqueous saturated NaCl (2×150 mL), dried over Na_2SO_4, and evaporated in vacuo to leave a yellow oil. The oil was redissolved in 100 mL H_2O, and acidified to pH = 1, and the aqueous solution washed with EtOAc (2×100 mL). The aqueous phase was basified to pH = 12 and the product extracted into EtOAc (3×100 mL). The organic layers were combined, washed with aqueous saturated NaCl (2×150 mL), dried over Na_2SO_4, and evaporated in vacuo to leave 2.0 g of crude product. The crude material was purified by flash chromatography using three eluants in the following order: Hexane:EtOAc (80:20), EtOAc (100%), MeOH (100%), to give 1.8 g of **6** as a yellow oil. ^{1}H NMR (500 MHz, CD_3OD): δ 8.17 (d, $J = 10$ Hz, 2H), 7.53 (d, $J = 10$ Hz, 2H), 3.63 (s, 2H), 2.38 (t, $J = 15$ Hz, 4H), 1.5–1.4 (m, 4H), 0.86 (t, $J = 15$ Hz, 6 H); ^{13}C NMR (125 MHz, CD_3OD): δ 150.2, 148.9, 131.2, 124.8, 59.7, 57.8, 21.7, 12.7; HRMS (EI^+): calcd 237.1606, found 237.1603.

***N*-(4-Nitrobenzyl)-dipropyl-*N*-oxide (7).** *N*-(4-Nitrobenzyl)-dipropylamine **6** (0.20 g, 0.85 mmol) was dissolved in 20 mL of CH_2Cl_2 and the solution brought to 0 °C. After addition of mCPBA (50–60%, 0.16 g, 0.93 mmol) the solution was stirred for 1 h at 0 °C, then 4 h at room temperature. Evaporation of the CH_2Cl_2 left the crude product which was redissolved in 50 mL H_2O and

brought to pH = 12 using saturated sodium carbonate. The aqueous phase was extracted with CH_2Cl_2 (3×50 mL) and the organic layers combined, washed with aqueous saturated NaCl (2×150 mL), dried over Na_2SO_4, and evaporated in vacuo to leave 60.0 mg of crude solid. Purification of the crude material by flash chromatography was accomplished using four mobile phases in the following order: EtOAc:hex (50:50), EtOAc (100%), MeOH (100%), MeOH:$CHCl_3$ (90:10). The product **7** (70.0 mg, 33%) was obtained as a white solid. ^{1}H NMR (500 MHz, CD_3OD): δ 8.26 (d, J = 12 Hz, 2H), 7.85 (d, J = 12 Hz, 2 H), 4.47 (s, 2H), 3.0–3.15 (m, 4H), 1.9–1.7 (m, 4 H), 0.95 (t, J = 15 Hz, 6H); ^{13}C NMR (125 MHz, CD_3OD): δ 150.6, 138.9, 135.5, 124.7, 70.1, 68.8, 18.1, 11.6; HRMS (EI^+): calcd 253.1546, found 253.1552.

Butyl-ethyl-(4-nitrophenyl) phosphate (8). Ethyl dichlorophosphate (1.0 g, 6.14 mmol) was dissolved in 10.0 mL CH_2Cl_2 and Et_3N (2.56 mL, 18.42 mmol) was added. *para*-Nitrophenol (0.854 g, 6.14 mmol) was dissolved in another 10.0 mL CH_2Cl_2 and added dropwise to the vigorously stirring reaction mixture over 10 min and allowed to stir at rt for 20 h. Afterward, 1-butanol (0.454, 6.14 mmol) was added in one portion and stirring continued for another 15 h. The reaction mixture was evaporated under reduced pressure then purified by flash chromatography and preparative TLC using EtOAc:hex (50:50) as eluant to give 0.38 g (20%) of **8** as a yellow oil. ^{1}H NMR (300 MHz, $CDCl_3$) δ 8.22 (d, J = 9 Hz, 2H), 7.35 (d, J = 9 Hz, 2H), 4.14–4.26 (m, 4 H), 1.63–1.69 (m, 2H), 1.33–1.42 (m, 4H), 0.91 (t, J = 7 Hz, 3H); ^{13}C NMR (125 MHz, $CDCl_3$): δ 155.8, 144.9, 125.9, 120.7, 69.1, 65.4, 32.4, 18.8, 16.3, 13.7; HRMS (Fab^+): calcd 304.0950, found 304.0946.

Dibutyl-(4-nitrophenyl) phosphate (9). 4-Nitrophenyl phosphorodichloridate (1.0 g, 3.91 mmol) was dissolved in 20.0 mL CH_2Cl_2 and Et_3N (1.2 mL, 8.6 mmol) was added. 1-Butanol was added in one portion at room temperature, and the reaction mixture stirred for 23 h. The reaction mixture was evaporated under reduced pressure then purified by flash chromatography using the mobile phase EtOAc:hex (50:50) to give 0.75 g (65%) of product **9** as a yellow oil. ^{1}H NMR (300 MHz, $CDCl_3$) δ 8.17 (d, J = 9 Hz, 2H), 7.32 (d, J = 9 Hz, 2H), 4.12 (dt, J = 6 Hz, 6 Hz, 4H), 1.63 (tt, J = 6 Hz, 7 Hz, 4H), 1.34 (dq, J = 6 Hz, 6 Hz, 4H), 0.87 (t, J = 7 Hz, 6H); ^{13}C NMR (125 MHz, $CDCl_3$): δ 155.8, 144.7, 125.7, 120.6, 68.9, 32.1, 18.6, 13.6; HRMS (FAB+): calcd. 332.1263, found 332.1258.

Acknowledgements

This work was supported in part by the National Institutes of Health (GM 43858), and an Individual National Research Service Award to D.A.S. (NIGMS GM17822).

References and Notes

1. Ecobichon, D. J. In *Casarett and Doull's Toxicology: The Basic Science of Poisons*, 4th ed.; Amdur, M. O.; Doull, J.; Klaasen, C. D.; Eds.; McGraw-Hill: New York, 1991; p 565.
2. Ember, L. *Chem. & Eng. News* **1997**, *75*, 26.
3. LeJeune, K. E.; Wild, J. R.; Russel, A. J. *Nature* **1998**, *395*, 27.
4. Cheng, T. C.; Calomiris, J. J. *Enzyme Microb. Technol.* **1996**, *18*, 597.
5. LeJeune, K. E.; Russel, A. J. *Biotechnol. Bioeng.* **1996**, *51*, 450.
6. *Alternative Technologies for the Destruction of Chemical Agents and Munitions*, National Research Council on Engineering and Technical Systems, Washington D.C., **1993**.
7. Omburo, G. A.; Kuo, J. M.; Mullins, L. S.; Raushel, F. M. *J. Biol. Chem.* **1992**, *267*, 13278.
8. Lewis, V. E.; Nonarski, W. J.; Wilk, J. R.; Raushel, F. M. *Biochemistry* **1988**, *27*, 1591.
9. Caldwell, S. R.; Newcomb, J. R.; Schlect, K. A.; Raushel, F. M. *Biochemistry* **1991**, *30*, 7438.
10. Butler, V. P., Jr. *Pharmacol. Rev.* **1982**, *34*, 109.
11. Carrera, M. R.; Ashley, J. A.; Parsons, L. H.; Wirsching, P.; Koob, G. F.; Janda, K. D. *Nature* **1995**, *378*, 727.
12. Rosenblum, J. S.; Lo, L.-C.; Li, T.; Janda, K. D.; Lerner, R. A. *Angew. Chem.* **1995**, *107*, 2448; *Angew. Chem., Int. Ed. Engl.* **1995**, *34*, 2275.
13. Lavey, B. J.; Janda, K. D. *Bioorg. Med. Chem. Lett.* **1996**, *6*, 1523.
14. Lavey, B. J.; Janda, K. D. *J. Org. Chem.* **1996**, *61*, 7633.
15. Tramantano, A.; Janda, K. D.; Lerner, R. A. *Science* **1986**, *234*, 1566.
16. Tanaka, F.; Linoshita, K.; Tanimura, R.; Fujii, I. *J. Am. Chem. Soc.* **1996**, *118*, 2332.
17. Li, T.; Hilton, S.; Janda, K. D. *J. Am. Chem. Soc.* **1995**, *117*, 2123.
18. Gibbs, R. A.; Benkovic, P. A.; Janda, K. D.; Lerner, R. A.; Benkovic, S. J. *J. Am. Chem. Soc.* **1992**, *114*, 3528.
19. Caldwell, S. R.; Raushel, F. M.; Weiss, P. M.; Cleland, W. W. *Biochemistry* **1991**, *30*, 7444.
20. Knowles, J. R. *Ann. Rev. Biochem.* **1980**, *49*, 877.
21. Khan, S. A.; Kirby, A. J. *J. Chem. Soc. B.* **1970**, 1172.
22. Lerner, R. A.; Benkovic, S. J.; Schultz, P. G. *Science* **1991**, *252*, 659.
23. Janda, K. D.; Chen, Y.-C. J. *The Pharmacology of Monoclonal Antibodies, Vol. 113*, Springer, Berlin, **1994**, 209.
24. Chen, Y.-C. J.; Janda, K. D. *J. Am. Chem. Soc.* **1992**, *114*, 1488.
25. Moriarty, R. M.; Hiratake, J.; Liu, K. *J. Am. Chem. Soc.* **1990**, *112*, 8575.
26. Shokat, K.; Uno, T.; Schultz, P. G. *J. Am. Chem. Soc.* **1994**, *116*, 2261.
27. Khalaf, A. I.; Proctor, G. R.; Suckling, C. J.; Bence, L. H.; Irvine, J. I.; Stimson, W. H. *J. Chem. Soc. Perkin Trans. 1* **1992**, 1475.
28. Janda, K. D.; Weinhouse, M. I.; Dannon, T.; Pacelli, K. A.; Schloeder, D. M. *J. Am. Chem. Soc.* **1991**, *113*, 5427.
29. Janda, K. D. *Biotechnol. Prog.* **1990**, *6*, 178.
30. Köhler, G.; Milstein, C. *Nature* **1975**, *256*, 495.
31. Lienhard, G. E. *Science* **1973**, *180*, 149–154.
32. Marsh, F. J.; Weiner, P.; Douglas, J. E.; Kollman, P. A.; Kenyon, G. L.; Gerlt, J. A. *J. Am. Chem. Soc.* **1980**, *102*, 1660.
33. Janda, K. D.; Weinhouse, M. I.; Schloeder, D. M.; Lerner, R. A.; Benkovic, S. J. *J. Am. Chem. Soc.* **1990**, *112*, 1274.